2000 IEEE/EIA International Frequency Control Symposium and Exhibition

LASER-COOLED RB CLOCK

Chad Fertig, Jérémie Bouttier, and Kurt Gibble, Yale University, New Haven, CT

ABSTRACT

We demonstrate a prototype of a laser-cooled ^{87}Rb fountain clock and measure the frequency shift due to cold collisions. The shift is fractionally 30 times smaller than that in a laser-cooled Cs clock. We observe a density dependent pulling by the microwave cavity and use it to cancel the collision shift. We have also demonstrated a juggling atomic fountain to study cold collisions and we discuss the importance of juggling for future fountain clocks.

1. INTRODUCTION

The most serious systematic error in laser-cooled clocks is the frequency shift due to cold collisions.[1] Tiesinga *et al.* first calculated this shift[2] and Gibble and Chu[3] measured the shift for laser-cooled Cs clocks to be $\delta\nu/\nu = -1.7\times10^{-12}$ at a density of 10^9 cm^{-3}. Due to Cs_2 molecular bound states near zero energy, the frequency shift cross section has nearly the maximal value of $\lambda_{dB}^2/2\pi$ where λ_{dB} is the de Broglie wavelength. This large cross section led us to examine clocks based on other atoms, for which the cold collision shift might be smaller.[4,5]

We measure the cold collision shift for ^{87}Rb and cancel the shift by detuning the microwave clock cavity. We have also demonstrated a juggling fountain. Juggling fountain clocks will be able to achieve higher stability without requiring large improvements in signal-to-noise (S/N) or the local oscillator. We discuss the optimal juggling rate and pattern that can cancel the frequency shift due to juggling collisions.

2. LASER-COOLED RB CLOCK

A schematic of our ^{87}Rb fountain clock is shown in Fig. 1. Using 0.9W of light from a Ti:Sapphire laser delivered by an optical fiber, atoms are collected from the room temperature Rb vapor in the vapor-cell MOT. The atoms are launched upwards and cooled to 1.8 μK in the moving frame. The atoms then pass through 2 microwave cavities that are normally used to prepare half of the atoms in the $5S_{1/2}$ $|F=1,m=0\rangle$ state.[6] Here, to achieve high density, the selection cavities are not used. Instead, we optically pump

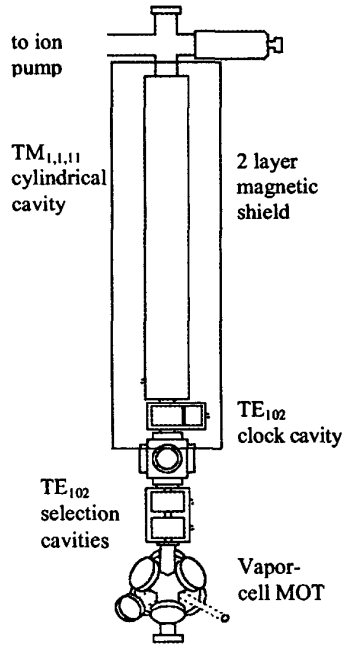

Figure 1. Schematic of ^{87}Rb fountain clock.

the atoms into $|1,-1\rangle$ just below the clock cavity. We use successive pulses of circularly polarized light from diode lasers tuned to the $5S_{1/2}$ $F=2 \rightarrow 5P_{3/2}$ $F'=1'$ and $1 \rightarrow 1'$ transitions. Microwaves from a horn then transfer atoms from $|1,-1\rangle$ state to the $|2,0\rangle$ state while a 35 mG horizontal magnetic field is applied along the direction of the optical pumping beams. A vertical magnetic field of 3.5 mG is then applied below the clock cavity as the horizontal bias field is switched off. Microwaves from the horn transfer a variable number of atoms from $|2,0\rangle$ to $|1,0\rangle$. Any atoms remaining in F=2 are cleared with light tuned to the $2\rightarrow3'$ transition. In this way, we can vary the density preparing a maximum of 70% of the atoms in $|1,0\rangle$ at a temperature of 5 μK with fewer than 1% in $|1,\pm1\rangle$. To prepare the atoms in $|2,0\rangle$, we add another microwave pulse to transfer the atoms in $|1,0\rangle$ to $|2,0\rangle$ and then repump any atoms in F=1 with light tuned to $1\rightarrow2'$.

The state prepared atoms enter the magnetic shielding and experience a 6.8 GHz microwave pulse in the rectangular TE_{102} clock cavity, creating a coherent

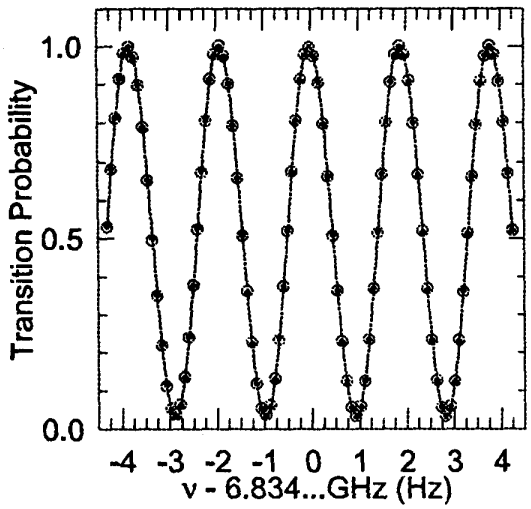

Figure 2. ^{87}Rb Ramsey fringes at 6.834 GHz. The large circles are the data and the small are a fit to the data. The linewidth is 0.95 Hz and the S/N=200.

superposition of $|1,0\rangle$ and $|2,0\rangle$. This coherence precesses as the atoms are slowed by gravity and return through the clock cavity. The second microwave pulse converts the phase difference between the atomic coherence and the microwave field into a population difference. We detect the transition probability using a laser tuned to $2\rightarrow3'$ producing Ramsey fringes as in Fig. 2. To normalize the fringes, we also detect the total number of atoms by repumping the population in $|1,0\rangle$ using a laser beam tuned $1\rightarrow2'$, followed by a second detection laser pulse. In Fig. 2, the interrogation time is T=0.526 s which gives a linewidth of $\Delta\nu$=0.950 Hz. With our detection signal-to-noise S/N=500 on a single launch, the atomic transition frequency[7] of 6,834,682,610.9 Hz can be determined in 1 s with a precision of $\delta\nu/\nu=\Delta\nu/\pi\nu S/N=9\times10^{-14}$. However, the short-term instability of our local oscillator limits the S/N to 200 or $\delta\nu/\nu=2.1\times10^{-13}$ for 1s of averaging. The magnetic bias field is 710 μG in the cavity and flight region which we probe by exciting a $\Delta m=1$ (sigma) transition in the cylindrical $TM_{1,1,11}$ cavity. The fractional quadratic Zeeman shift[1] for this field is $\delta\nu/\nu = 4\times10^{-14}$.

During the precession time above the clock cavity, collisions between cold atoms shift the phase of their coherence producing a frequency shift of the clock. To measure this frequency shift, we vary the atomic density on successive fountain launches and look for a relative shift of the Ramsey fringes. In Fig. 3 we show a series of measurements of the frequency as a function of density(circles) for atoms prepared in both $|1,0\rangle$ and $|2,0\rangle$. The extrapolated shift for a density of $1.0(6)\times10^9$ cm^{-3} is −0.38(8) mHz.[8,9] We also show the shift for Cs which is fractionally 30 times larger.[3] The measured shift agrees with that calculated in Ref. [5] and also a recent reanalysis of the ^{87}Rb interactions.[10,11]

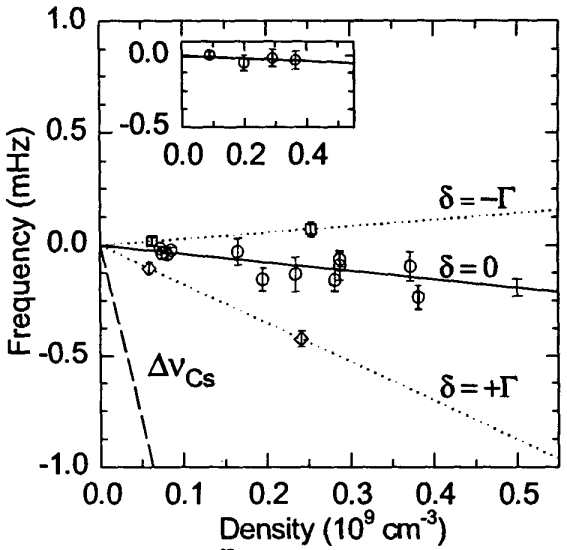

Figure 3. Measured ^{87}Rb cold collision shift (circles and solid line). The shift is -0.38(8) mHz for a density of $1.0(6)\times10^9$ cm^{-3}. The dashed line is the measured shift for Cs.[3] The dotted lines (diamonds and squares) show the density dependence for clock cavity detunings of $\delta=\pm\Gamma$. The inset shows a cancelled collision shift for δ = -30 kHz and atoms prepared in $|1,0\rangle$.

The measured frequency differences in Fig. 3 have a precision of $\pm2\times10^{-15}$. At the 10^{-15} level, there are several potential error sources. The only source that is explicitly density dependent is the pulling of the transition frequency by the coupling of the atoms to the microwave cavity.[12] In NMR, the effect is known as radiation damping where the field radiated by the magnetization of the sample builds up in the microwave cavity and causes the Bloch vector to decay.[13] In hydrogen masers, it is called cavity pulling and is used to cancel the collisional frequency shift.[14] Here, more apparent than the decay of the atomic coherence is a small phase shift. When the cavity is detuned from the atomic transition frequency, the field radiated by the atoms is phase shifted relative to the applied field. The Bloch vector precesses about the total field leading to a phase error proportional to $\mu_0\hbar\mu_B^2N\omega\delta/(\delta^2+\Gamma^2)V_{cav}$.[15,16] Here, N is the number of atoms, ω is the transition frequency, δ is the cavity detuning, Γ is the cavity HWHM, V_{cav} is the effective cavity volume, and μ_B is the Bohr magneton.

In Fig. 3 we also show the measured density dependent frequency shift when we detune the clock cavity by ±Γ for atoms prepared in $|1,0\rangle$ (diamonds and squares). The cavity detuning can significantly influence the density dependence. By detuning the cavity, we cancel the cold collision shift.[16] This spin-exchange tuning[14] has advantages for insuring immunity to long-term variations in the number of trapped atoms. Moreover, density

extrapolations can be more accurate since the extrapolation does not depend on accurate density ratios.[4]

The cavity pulling has several unique dependences that we observe. For example, the cavity pulling not only reverses with the cavity detuning δ but also with the initial population inversion of $|1,0\rangle$ and $|2,0\rangle$. In addition, the cavity pulling depends on the transition probability during each cavity passage. For a 0.5 transition probability on the first interaction($\pi/2$ pulse), a positive cavity detuning δ pulls the frequency higher (lower) for atoms prepared in $|2,0\rangle$ ($|1,0\rangle$). On the second $\pi/2$ pulse, if the microwave frequency is tuned to the side of a Ramsey fringe, the microwave field is phase shifted by $\pi/2$ so that it is parallel or anti-parallel to the Bloch vector. Therefore, the Bloch vector does not precess and the cavity pulling has no first order effect during the second interaction. For a transition probability of 0.25 in the first passage (0.33π pulse), the cavity pulls in the same direction during both cavity passages since the Bloch vector precesses during both. However, the effect of the second passage is small because the number of atoms is 8 times less due to their ballistic expansion. For a transition probability of 0.75 (0.67π pulse), the first cavity passage has a small effect as the Bloch vector is first perturbed in one direction as it precesses to $\theta=\pi/2$ and then the direction of the perturbation reverses once there is a population inversion. On the second passage, the perturbation remains reversed so that the total cavity pulling is small.

We show the cavity pulling effects in Fig 4. We plot the density dependent shift versus the atomic transition probability during the first cavity passage for $n=10^9$ cm^{-3}. For a cavity tuned below the atomic resonance, $\delta=-\Gamma$, and atoms prepared in $|1,0\rangle$, the frequency shift is positive and large for a small transition probability (open squares and dashed line). When the atoms are prepared in $|2,0\rangle$, the filled squares show a large negative density dependent shift for a small transition probability. The dotted line and open (filled) diamonds show the opposite density dependence for $\delta=+\Gamma$, and $|1,0\rangle$ ($|2,0\rangle$) state preparation.

To model the data in Fig. 4, we account for the different cold-collision frequency shifts λ_{10} and λ_{20} due to the $|1,0\rangle$ and $|2,0\rangle$ populations, and the cavity pulling. For no cavity pulling ($\delta=0$), we see essentially no shift as a function of the population in $|2,0\rangle$ during the precession time. We model the 18 measurements in Fig. 4 accounting for the partial frequency shift cross sections and the cavity pulling by integrating the time evolution of the Bloch vector as the atom passes through the microwave field profile of the clock cavity. The model agrees and we find $2(\lambda_{10}-\lambda_{20})/(\lambda_{10}+\lambda_{20})=0.1(6)$. This constrains a determination of the ^{87}Rb interactions that suggests either -1.63 or 0.08.[10]

Although cavity pulling and the cold collision shift are the only systematic errors that explicitly depend on the atomic density, it is important to control all errors near the level of 10^{-15}. Our frequency reference is an ovenized 5

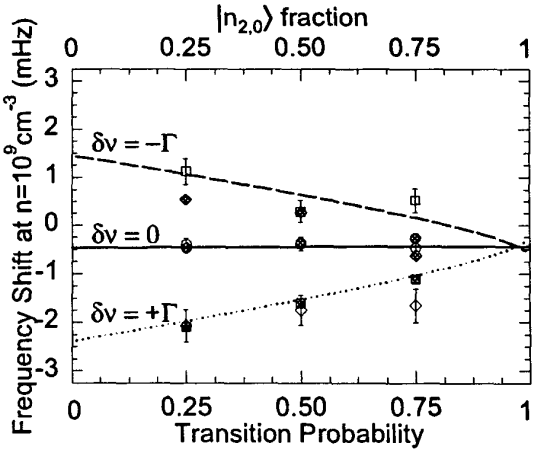

Figure 4. Density dependent shift versus transition probability on a single clock cavity passage for clock cavity detunings of $\delta=+\Gamma$ (diamonds and dotted) and $-\Gamma$ (squares and dashed line). Open (filled) data points are for atoms prepared in $|1,0\rangle$ ($|2,0\rangle$). For $\delta=0$, the circles and solid line are plotted versus the fraction of atoms in $|2,0\rangle$ in the fountain, giving the individual shift contributions from $|1,0\rangle$ and $|2,0\rangle$ state populations. Typical error bars are shown for open points.

MHz quartz BVA oscillator that is successively frequency multiplied and mixed with a low frequency synthesizer to make 6834.6 MHz. Considerable care is taken to avoid line pulling by spurious frequencies and 60 Hz phase modulation.[17] We test for line pulling and microwave leakage by observing the clock frequency while driving $\pi/2$, $3\pi/2$... $11\pi/2$ pulses and also adjust the fringe space to be most sensitive to 60Hz harmonics. These effects are below 8×10^{-16} and the density dependent component is below 1×10^{-16}.

Inhomogeneities in the state preparation can combine with other errors, such as the distributed cavity phase shift, to mimic a density-dependent frequency shift. To exaggerate this effect, we select atoms with $\pi/2$, ... $9\pi/2$ pulses from the microwave horn as shown in Fig. 5. Thus, any small gradient in the selection would be 8 times larger for a $9\pi/2$ than for $\pi/2$ selection. We fit the measured frequencies versus $N\pi/2$ to a mean frequency and an alternating term proportional to N. For a $\pi/2$ pulse, the shift is less than 7×10^{-16}. Further, we take data by selecting 1/4 of the atoms with both 0.3π and 1.7π pulses so that any selection gradient is reversed.

Another spatially inhomogeneous shift is the quadratic Zeeman shift from the 710 μG bias field. The shift of the clock's frequency is 4.3×10^{-14}. Over the top 4 cm of the fountain, the field is homogeneous over the volume sampled by the atoms to 1 μG and the gradient is less than 20 μG/cm producing systematic errors less than 1×10^{-16}. Finally, we check for an AC Stark shift due to the lasers

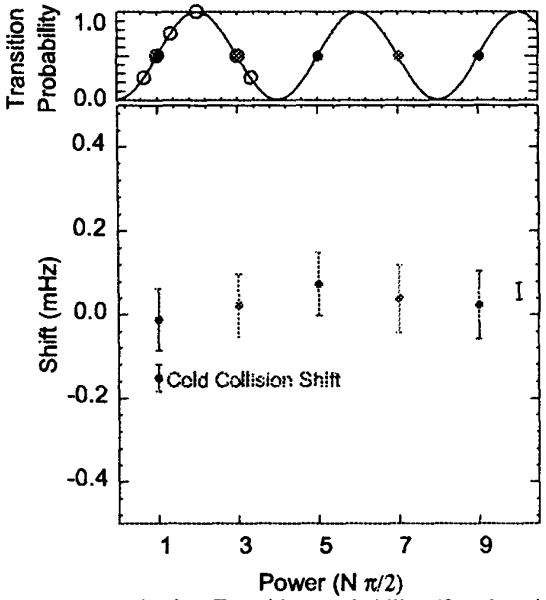

Figure 5. Selection Transition probability (for changing the density) and clock frequency versus power to the selection microwave horn. The fitted uncertainty is shown (rightmost point). After dividing it by 8, it is negligible when compared to the measured collision shift. For the collision shift measurements, we select atoms with a variety of pulses from 0.33π to 1.7π (open circles in the upper graph)to further reduce any inhomogeneous selection effects.

and find the density dependent component to be below 2×10^{-16}.

The atomic density is measured using laser absorption. An attenuated 1mm laser beam is apertured, aimed vertically through the center of the clock cavity, and then centered on the ball of atoms. We frequency scan a 50μs pulse over 40 MHz near the $2 \rightarrow 3'$ transition at 9 times throughout the fountain trajectory. We measure the vertical size of the atomic sample on the upward and downward passages through the detection region, with and without state preparation. We model the evolution of the atomic density as a ballistic expansion of uncorrelated Gaussian velocity and spatial distributions and account for the heat added during the state preparation. This produces a density as a function of time as shown in Fig. 6. We calculate the time-averaged density for the atoms that we detect below the clock cavity (dashed line in Fig. 6). This effective density depends on the transverse velocity and spatial distributions, and we extract this information from the time evolution of the vertical optical thickness of the sample. Without independent corroboration, it is difficult to be certain about the absolute density scale to better than 60%. With quantitative and absolute tests of our model of cavity pulling, the cavity pulling could be used to measure accurately and independently the atomic density.[18]

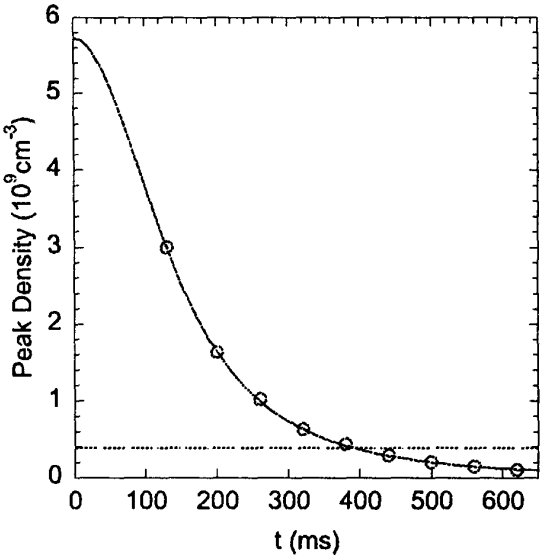

Figure 6. Peak transverse density as a function of time. The temporally and spatially averaged density is shown as a dashed line.

We tune the clock cavity by $\delta=\pm\Gamma$ by changing its temperature by $\mp$2.5K. To measure the frequency response of the cavity we detect the AC Zeeman shift of the clock states due to a strong microwave sideband that is injected into the clock cavity.[6] In Fig 7, we show the shift of the clock transition (inset) and and the inferred response of the cavity. The loaded Q of our TE_{102} copper clock cavity is 13,000 and it is tuned with an accuracy of 5 kHz.

3. JUGGLING CLOCKS

One can achieve higher stabilities and eliminate the dead time (reducing the requirements for the local reference oscillator) by *juggling* atoms in the fountain as shown in Fig. 8. With a S/N = 2300 on a single launch, the frequency uncertainty would be $\delta\nu/\nu = \Delta\nu/(\pi\ \nu\ S/N) = 2\times10^{-14}$. If the cycle time is 1 s, then the fractional instability of the clock after 1s of averaging is $\sigma_y(\tau=1s) = 2\times10^{-14}\tau^{-1/2}$. By launching balls of atoms at a rate of 25 s^{-1}, the dead time is eliminated and gives a short-term instability of $\sigma_y(\tau) = 4\times10^{-15}\tau^{-1/2}$. This improvement is achieved without the technical difficulty of higher S/N and higher atomic densities. There are 2 important problems: 1) shutters, as shown in Fig. 8, must be used to block the trapping and cooling light from the interrogation region of the clock; 2) collisions between juggled balls of atoms will shift the frequency of the clock.

We have demonstrated a juggling Cs fountain and have studied collisions between 2 balls of atoms.[19] In this experiment we observe the velocity changes rather than a

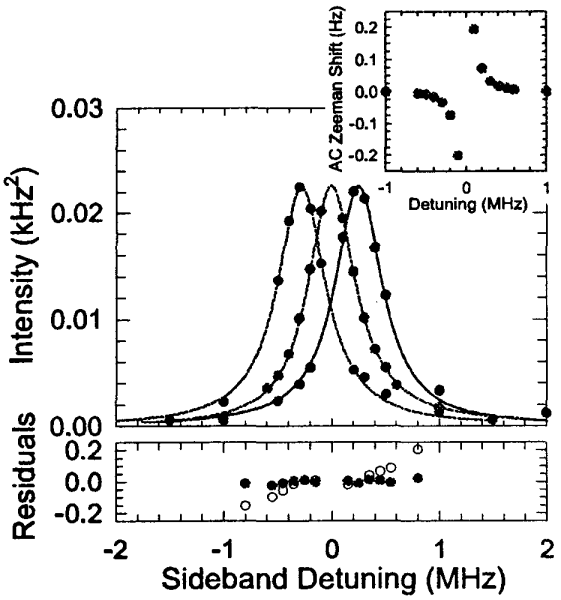

Figure 7. Cavity response versus sideband frequency for 3 temperatures. The cavity response is measured using the AC Zeeman shift of the clock transition due to a microwave sideband (inset). The residuals of the δ=0 fit have an asymmetry due to the TE_{101} waveguide feed cavity (open circles). Accounting for it, the residuals are 1% or 0.04 dB (filled circles).

phase shift of an atomic coherence. We rapidly launch 2 balls of atoms from a double-MOT[20] at the same velocity. The relative velocity is then $v_r = \Delta T \times g$ where ΔT is the delay between launches. Here, ΔT = 7 ms $\rightarrow$ 20 ms corresponds to collision energies of 19 to 150 μK. This range of energies is interesting as one expects to see the p-wave quantum scattering threshold – at low energies only s-wave scattering occurs since, for impact parameters that are within the range of the interatomic potential, the velocity is low enough that the angular momentum is less than $\hbar$. As the energy increases to about 30 μK, there is enough angular momentum for impact parameters within the potential to have ℓ=1.[21]

To be sensitive to the differential cross section, we detect the vertical velocity component of the scattered atoms using a 2-photon Raman transition.[20,22] In Fig. 9, we show the Cs s & p-wave cross-sections as a function of energy. At low energies, the s-wave cross section, which is pure triplet scattering, becomes constant. The p-wave cross section increases as the square of the energy for low energies as expected for a p-wave scattering threshold and then rolls over at higher energies. Since the p-wave channel is an admixture of singlet and triplet interactions, we can get a great deal of detailed information about the Cs-Cs scattering at low energies. The s-wave data determines the triplet potential allowing the p-wave to determine the

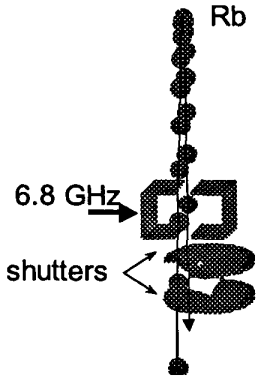

Figure 8. Schematic for a juggling fountain clock. Balls of laser-cooled atoms are launched faster than the flight time above the microwave cavity.

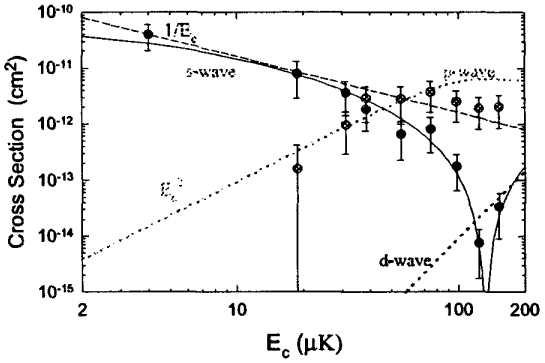

Figure 9. Energy dependence for s & p-waves cross sections. For reference, we show lines corresponding to 1/E and E^2 corresponding to an s-wave "resonance" and the p-wave quantum scattering threshold. At higher energies, the s-wave cross section goes to zero indicating a Ramsauer-Townsend minimum near 200 μK.

singlet. This experiment is the first to resolve the quantum scattering for atomic partial waves.

At higher energies, the s-wave cross section decreases to nearly zero indicating a s-wave Ramsauer-Townsend cross-section minimum[23] near 200 μK. The Ramsauer-Townsend effect can be used to minimize the cold collision shift in a juggling fountain clock. By carefully choosing the launch rate, one can minimize the effects of collisions between successive balls

In Fig. 10 we show a calculation of the s-wave juggling frequency shift for ^{87}Rb. The first null in the shift occurs at 0.12 mK corresponding to a time delay of 22 ms. Unfortunately, the peak of the s-wave juggling shift is very nearly at a time delay of 44 ms. Therefore, for a juggling rate of 1/(22 ms), the energy for collisions between every other ball would be near the peak of the juggling shift. To cancel the juggling shift, one can launch with a more sophisticated pattern. A pattern that cancels the s-wave

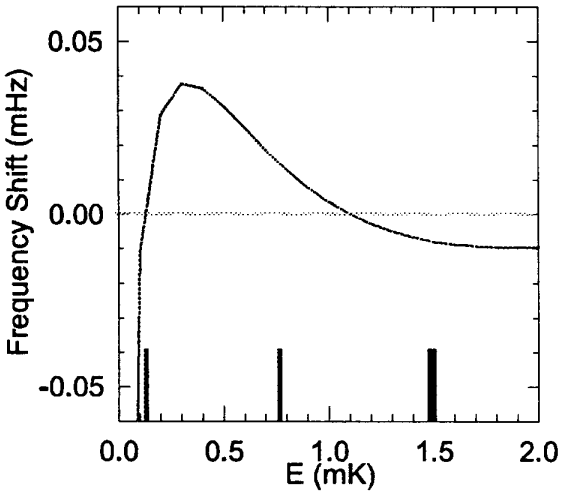

Figure 10. Juggling frequency shift for s-waves. The juggling shift is zero for time delays of 22ms (0.12mK) and 66 ms (1.1mK). The energy spectrum shown corresponds to juggling pattern depicted in Fig. 11.

shift launches balls with alternate delays of 22 and 55 ms as shown in Fig. 11. The energy spectrum for this pattern is also shown in Fig. 10. Each ball collides with 1 ball with a 22 ms delay for which there is no shift. Each ball also collides with another at 55 ms delay, for which the shift is positive, and with 2 balls at 77 ms where the shift is negative and half as large as the shift at 55 ms. There is no p-wave shift due to Bose symmetry and higher partial waves will generally have random signs and all of the shifts decrease at higher energies. It is likely that a pattern similar to that in Fig. 11 will give a high juggling rate and cancel the total juggling collision shift.

4. CONCLUSIONS

We have demonstrated a prototype of an ^{87}Rb fountain clock. Varying the density, we see a small shift in the clock frequency that is fractionally 30 times smaller than the shift for a laser-cooled Cs clock. By detuning the microwave clock cavity, we cancel the shift. This will allow an ^{87}Rb clock to operate with a short-term stability of 2×10^{-14} for 1s of averaging with a cold collision shift of 2×10^{-16} that can be cancelled with an accuracy of 1×10^{-17}. Juggling atoms will increase the stability to 4×10^{-15} for 1s of averaging, giving an unprecedented combination of short-term stability and long-term accuracy. We have demonstrated a juggling Cs atomic fountain and observed the energy dependence for s & p-wave scattering, including the Ramsauer-Townsend effect. In a juggling clock, we can choose the juggling rate and pattern to utilize the Ramsauer minima so that the juggling frequency shift can be cancelled.

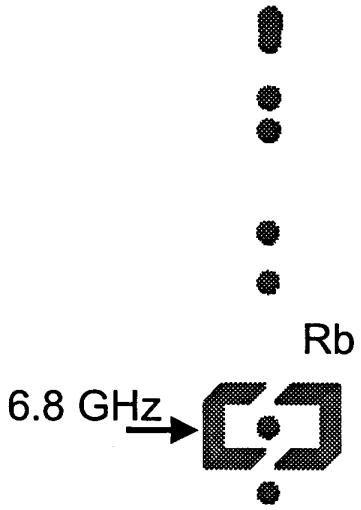

Figure 11. Juggling pattern of alternate launch delays of 22 and 55 ms to cancel the s-wave juggling frequency shift.

5. ACKNOWLEDGEMENTS

We acknowledge discussions with Servaas Kokkelmans, Boudewijn Verhaar, and Mike Hayden and financial support from the NASA Microgravity program, an NSF NYI award, and a NIST Precision Measurement Grant.

6. REFERENCES

1. See K. Gibble and S. Chu, Metrologia **29**, 201 (1993).
2. E. Tiesinga, B. J. Verhaar, H. T. C. Stoof, and D. van Bragt, Phys. Rev. A **45**, 2671 (1992).
3. K. Gibble and S. Chu, Phys. Rev. Lett. **70**, 1771 (1993).
4. K.Gibble and B. J. Verhaar, Phys. Rev. A **52**, 3370 (1995).
5. S. J. J. M. F. Kokkelmans, B. J. Verhaar, K. Gibble, and D. J. Heinzen, Phys. Rev. A. **56**, 4389 (1997).
6. C. Fertig and K. Gibble, IEEE Trans. Instr. Meas. **48**, 520 (1999).
7. S. Bize, Y. Sortais, M. S. Santos, C. Mandache, A. Clairon, and C. Salomon, Europhys. Lett, **45**, 558 (1999).
8. C. Fertig and K. Gibble, Phys. Rev. Lett. **85**, in press (2000).
9. See also S. Bize, Y. Sortais, C. Mandache, A. Clairon, and C. Salomon, submitted to Phys. Rev. Lett (2000).
10. S. Kokkelmans and B. J. Verhaar, private communication (2000).
11. Carl Williams, private communication (2000).

12. There is cavity pulling in Cs beam clocks due to the variation of the microwave power across the transition. This effect is easily eliminated in fountain clocks by working with 2 $\pi/2$ pulses and measuring more than the central Ramsey fringe.
13. S. Bloom, J. Appl. Phys. **28**, 800 (1957).
14. S. B. Crampton, Phys. Rev. **158**, 57 (1967).
15. M. E. Hayden and W. N. Hardy, J. Low Temp. Phys. **99**, 787 (1995).
16. C. Fertig, J. Bouttier, and K. Gibble, to be submitted to IEEE Trans. Instr. Meas.
17. A. De Marchi, G. D. Rovera, and A. Premoli, Metrol. **20**, 37 (1984).
18. Our cavity pulling model and our measured density are consistent to 10% with an uncertainty of at least 30%.
19. R. Legere and K. Gibble, Phys. Rev. Lett. **81**, 5780 (1998).
20. K. Gibble, S. Chang, and R. Legere, Phys. Rev. Lett **75**, 2666 (1995).
21. See P. S. Julienne and F. H. Mies, J. Opt. Soc. Am. B **6**, 2257 (1989).
22. M. Kasevich, D. S. Weiss, E. Riis, K. Moler, S. Kasapi, and S. Chu, Phys. Rev. Lett. **66**, 2297 (1991).
23. Ramsauer, Ann. der Physik **72**, 345 (1923); Townsend and Bailey, Phil. Mag. **43**, 593 (1922).